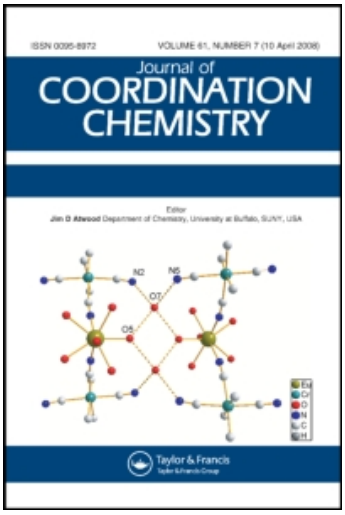

Journal of Coordination Chemistry
Publication details, including instructions for authors and subscription information:
http://www.informaworld.com/smpp/title~content=t713455674

The synthesis, spectroscopic and voltametric studies of new metal complexes containing three different *vic*-dioximes

Ahmet Kilic[a]; Esref Tas[a]; Bahattin Gumgum[b]; Ismail Yilmaz[c]
[a] Department of Chemistry, Harran University, Sanliurfa 63510, Turkey [b] Department of Chemistry, Dicle University, 21280 Diyarbakir, Turkey [c] Department of Chemistry, Technical University of Istanbul, 34469 Istanbul, Turkey

To cite this Article Kilic, Ahmet , Tas, Esref , Gumgum, Bahattin and Yilmaz, Ismail(2007) 'The synthesis, spectroscopic and voltametric studies of new metal complexes containing three different *vic*-dioximes', Journal of Coordination Chemistry, 60: 11, 1233 — 1246
To link to this Article: DOI: 10.1080/00958970601035914
URL: http://dx.doi.org/10.1080/00958970601035914

Journal of Coordination Chemistry
Vol. 60, No. 11, 20 July 2007, 1233–1246

Taylor & Francis
Taylor & Francis Group

The synthesis, spectroscopic and voltametric studies of new metal complexes containing three different *vic*-dioximes

AHMET KILIC†, ESREF TAS*†, BAHATTIN GUMGUM‡ and ISMAIL YILMAZ§

†Department of Chemistry, Harran University, Sanliurfa 63510, Turkey
‡Department of Chemistry, Dicle University, 21280 Diyarbakir, Turkey
§Department of Chemistry, Technical University of Istanbul, 34469 Istanbul, Turkey

(*Received 27 January 2006; revised 9 June 2006; in final form 13 June 2006*)

The synthesis, spectroscopic, and redox properties of some metal complexes with three novel *vic*-dioxime ligands, *N*-(1-(2-aminoethyl)piperazine)-phenylglyoxime (L_1H_2), *N*-(1-(2-aminoethyl)piperazine)-glyoxime (L_2H_2), and *N*,*N*′-*bis*(1-(2-aminoethyl)piperazine)-glyoxime (L_3H_2)], prepared from different glyoxime and 1-(2-aminoethyl)piperazine are reported. The structure of these *vic*-dioximes have been determined as the *anti*-form according to ^{1}H NMR, ^{13}C NMR, and FT-IR data. The metal to ligand ratios of Co(II), Ni(II), and Cu(II) complexes were found to be 1 : 2. The Cu(II) complexes of these ligands are proposed to be square planar and Ni(II) complexes of these ligands are proposed to be square planar or octahedral, while the Co(II) complexes are proposed to be octahedral with water molecules as axial ligands. Ni(II), Co(II), and Cu(II) metal complexes are non-electrolytes as shown by their molar conductivities (Λ_M) in DMF (dimethyl formamide) at 10^{-3} M. The structure of ligands and their complexes is proposed from elemental analysis, FT-IR, UV-VIS, ^{1}H NMR, ^{13}C NMR, magnetic susceptibility measurements, and molar conductivity measurements. The cyclic voltammetric measurements of the mononuclear complexes provide an understanding of the electrochemical behaviour of the reduced or oxidized species in DMSO solution.

Keywords: *vic*-dioxime; Metal complexes; Synthesis; Spectroscopy; Redox properties

1. Introduction

The synthesis of *vic*-dioximes and their different derivatives have been the subject of study for very a long period of time. Macromolecules attached to dioximes and their transition metal complexes have been investigated [1, 2]. The transition metal complexes of *vic*-dioximes have been of particular interest as biological model compounds [3]. Most of the work carried out so far as on symmetrically disubstituted [4–6] glyoximes and partly on mono-substituted ones [7, 8]. The dioxime ligands are known to coordinate metal ions as neutral dioximes and also as monoanionic dioximates via dissociation of one oxime proton [3, 9]. Coordination chemistry of the oxime ligands has been extensively studied with the 3d metal ions [10, 11]. When asymmetrical

*Corresponding author. Email: etas@harran.edu.tr

Journal of Coordination Chemistry
ISSN 0095-8972 print/ISSN 1029-0389 online © 2007 Taylor & Francis
DOI: 10.1080/00958970601035914

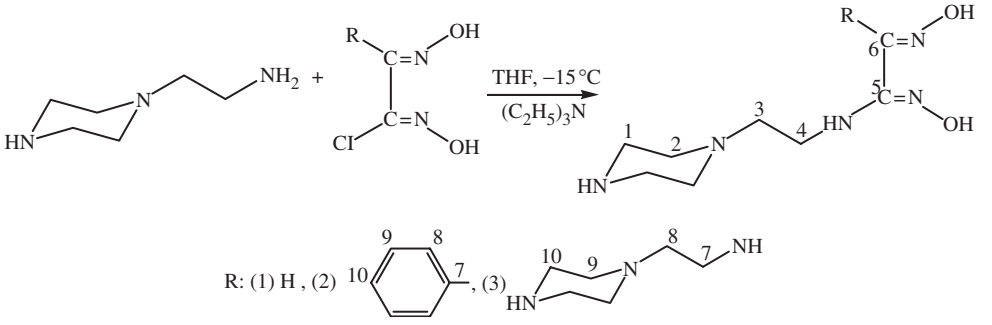

Scheme 1. Synthesis of L_1H_2, L_2H_2 and L_3H_2.

dioximes such as phenylglyoxime or methylglyoxime are employed as starting ligands, a mixture of *fac*- and *mer*-isomers was obtained. However, in some cases one of them was isolated individually [12]. Extensive studies of cobaloximes beginning in the 1960 s made use of $Co(DMGH)_2$ as a substitute for the naturally occurring cobalt corrin ring system [13, 14]. Dimethylglyoxime [3] is a well-known ligand commonly used in the analysis for nickel. The insoluble red $Ni(DMGH)_2$ complex was originally described by Tschugaev in 1905 [15]. Recently, metal containing oxime complexes have been utilized in medicine as well, technetium(V) and copper(II) complexes containing vicinal dioxime currently are used as cerebral and myocardial perfusion imaging agents [16]. Also, the two hydrogen bridges have been substituted with metal complexes to obtain polynuclear compounds in order to investigate the magnetic interactions [17].

The aim of the present study was to synthesize and characterize three novel dioxime (scheme 1) containing 1-(2-aminoethyl)piperazine and to obtain their mononuclear complexes with Co(II), Cu(II), and Ni(II) ions (figure 1). The cyclic voltammetric measurements of the mononuclear complexes have also been studied to understand electrochemical behaviour of their reduced or oxidized species in nonaqueous solution.

2. Experimental

All reagents and solvents were of reagent-grade quality and obtained from commercial suppliers. (Fluka Chemical Company, Taufkirchen, Germany) and tetra-*n*-butylammonium perchlorate (*n*-Bu_4NClO_4, Fluka Chemical Company, Taufkirchen, Germany) were used as received. *Anti*-phenylchloroglyoxime was synthesized as described in the literature, [18] *anti*-monochloroglyoxime was synthesized as described in the literature [19, 20], and (*E, E*)-dichloroglyoxime was prepared by a reported procedure [21, 22]. The elemental analyses were carried out in the Laboratory of the Scientific and Technical Research Council of Turkey (TUBITAK). IR spectra were recorded on a Perkin-Elmer Spectrum RXI FT-IR Spectrometer as KBr pellets. ^{1}H-NMR and ^{13}C-NMR spectra were recorded on a Bruker-Avence 400 MHz spectrometers. Magnetic Susceptibilities were determined on a Sherwood Scientific Magnetic Susceptibility Balance (Model MK1) at room temperature (20°C) using $Hg[Co(SCN)_4]$ as a calibrant; diamagnetic corrections were calculated from Pascal's constants [20]. UV-VIS spectra were recorded on a Schimadzu 1601 PC.

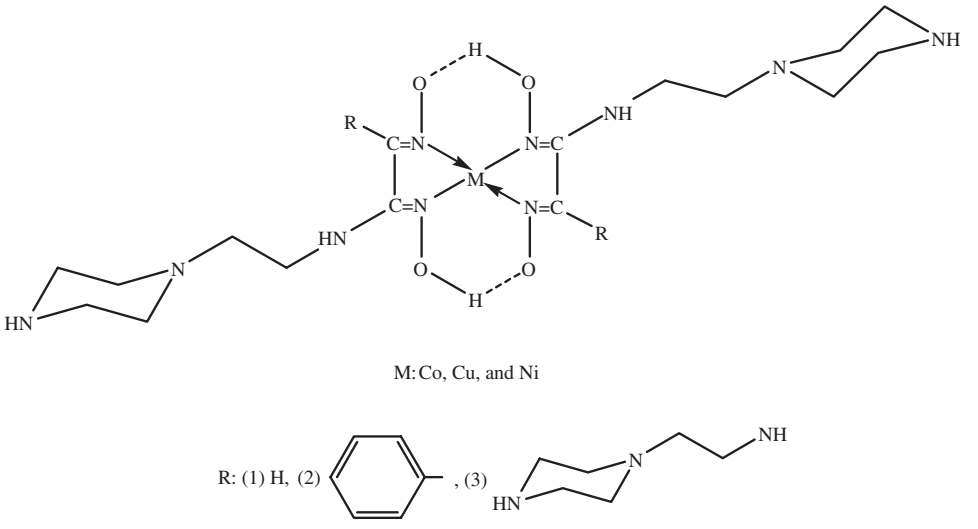

Figure 1. The structure of the Co(II), Cu(II), and Ni complexes.

Molar conductivities (Λ_M) were recorded on a Inolab Terminal 740 WTW Series. An EcoChemie Autolab-12 potentiostat with the electrochemical software package GPES 4.9 (Utrecht, The Netherlands) was used for voltammetric measurements. A three electrode system was used: a platinum wire counter electrode, an Ag/AgCl reference electrode and a 2 mm sized platinum disc electrode as working electrode. The working electrode was polished with 0.05 μm alumina prior to each experiment. Throughout the experiment, oxygen-free nitrogen was bubbled through the solution for 10 min. Voltammetric experiments were performed at room temperature. Electrochemical grade tetrabutylammonium perchlorate (TBAP) (0.1 mol dm^{-3}) was employed as the supporting electrolyte.

2.1. *Synthesis of the ligands L_1H_2, L_2H_2, and L_3H_2*

1-(2-Aminoethyl)piperazine (1.29 g, 10 mmol for L_1H_2, 1.95 g, 15 mmol for L_2H_2, and 2.58 g, 20 mmol for L_3H_2, respectively) was dissolved in 60 cm^3 absolute tetrahydrofuran (THF). Then triethylamine (Et_3N) (1.01 g, 10 mmol for L_1H_2, 1.52 g, 15 mmol for L_2H_2, and 2.02 g, 20 mmol for L_3H_2, respectively) was added and the mixture was cooled to −15°C and kept at this temperature. To this solution, *anti*-phenylchloroglyoxime (1.99 g, 10 mmol), *anti*-monochloroglyoxime (1.84 g, 15 mmol) or *anti*-dichloroglyoxime (1.57 g, 10 mmol) in 30 cm^3 absolute tetrahydrofuran (THF) was added dropwise under a N_2 atmosphere with continuous stirring. The addition of the *anti*-phenylchloroglyoxime, *anti*-monochloroglyoxime or *anti*-dichloroglyoxime solutions were carried out during 3 h. The mixture was stirred for more than 2 h and the temperature was raised to 25°C. Precipitated Et_3NHCl was filtered off and the filtrate was evaporated to remove THF. The oily products were dissolved in CH_2Cl_2 (10 cm^3) and *n*-hexane (125 cm^3) added to precipitate the compounds. This process was then repeated several times. But, the L_3H_2 ligand was not purified. Ligands (L_1H_2 and L_2H_2) were filtered and dried in a vacuum. Ligands are

soluble in common organic solvents such as THF, EtOH, and DMSO, whereas their metal complexes are soluble only in DMSO and DMF. L_1H_2 of characteristic ^{1}H-NMR, the chemical shift (DMSO-d_6, TMS, δ: ppm): 11.40 (b, 2H, OH), 5.80–5.62 (d, 1H, NH), 7.80–7.30 (m, 5H, Ar–CH), 3.20–2.60 (m, 6H, NH–CH_2), 2.55–2.10 (m, 6H, N–CH_2). L_2H_2 of characteristic ^{1}H-NMR, the chemical shift ($CDCl_3$-d_1, TMS δ: ppm): 10.14 (s, 1H, OH) and 10,52 (s, 1H, OH), 5.54 (s, 1H, NH), 7.92 (s, 1H, HC=N), 2.49–2.32 (t, 4H, NH–$^1CH_2$), 3.49–3.04 (m, 4H, NH–$^4CH_2$ and N–$^3CH_2$), 0.93–0.90 (t, 6H, N–$^2CH_2$). L_2H_2 of characteristic ^{13}C-NMR, the chemical shift (DMSO-d_6, TMS, δ: ppm): C_6(139.0), C_5(153.7), C_4(46.3), C_3(48.4), C_2(52.9) and C_1(58.9).

2.2. *Synthesis of the metal complexes*

2.2.1. Metal complexes of L_1H_2 and L_2H_2. A solution of nickel(II) chloride hexahydrate (0.12 g, 0.5 mmol), cobalt(II) chloride hexahydrate (0.12 g, 0.5 mmol), and copper(II) chloride dihydrate (0.085 g, 0.5 mmol) in ethanol (20 cm^3) were added to a solution of L_1H_2 (0.3 g, 1 mmol) and L_2H_2 (0.22 g, 1 mmol) in ethanol (75 cm^3) at 60–65°C. A distinct change was observed in colour from colourless to red, brown and green under a N_2 atmosphere with continuous stirring. Then, a decrease in the pH of the solution was observed. The pH of the solution was ca 1.5–3.0 and was adjusted to 4.5–5.5 by the addition of a 1% NaOH solution in EtOH. After heating the mixture for 2 h in a water bath, the precipitate was filtered off, washed with H_2O and diethyl ether several times, and dried *in vacuo*. [Ni(L_1H)$_2$] of characteristic ^{1}H-NMR. The chemical shift (DMSO-d_6, TMS, δ: ppm): 15.62 (b, 2H, O−H · O), 5.76 (s, 2H, NH), 7.76–7.42 (m, 10H, Ar–CH), 3.43–2.74 (m, 12H, NH–CH_2), 2.81–2.25 (m, 12H, N–CH_2) and [Ni(L_2H)$_2$] of characteristic ^{1}H-NMR, the chemical shift (DMSO-d_6, TMS, δ: ppm) δ: 14.42 (s, 2H, O−H · O), 5.31 (s, 2H, NH), 8.06 (s, 2H, HC=N), 3.76–2.94 (m, 12H, NH–CH_2), 2.79–2.31 (m, 12H, N–CH_2).

2.2.2. Metal complexes of L_3H_2. Dichloroglyoxime (0.50 g, 3.2 mmol) was dissolved in 30 cm^3 absolute ethanol. Then, $NiCl_2 \cdot 6H_2O$ (0.38 g, 1.6 mmol), $CoCl_2 \cdot 6H_2O$ (0.38 g, 1.6 mmol) or $CuCl_2 \cdot 2H_2O$ (0.27 g, 1.6 mmol) in 15 cm^3 absolute ethanol was added dropwise under a N_2 atmosphere with continuous stirring. To this solution, 1-(2-aminoethyl)piperazine (1.10 g, 8.5 mmol) in 20 cm^3 absolute ethanol was added dropwise under a N_2 atmosphere. The stirred mixture was then heated to the reflux temperature and was maintained at this temperature for 3 h. The pH of a solution was ca 1.5–3.0 and was adjusted to 4.5–5.5 by the addition of a 1% NaOH solution in ethanol. After cooling to room temperature, the complexes were filtered, washed with H_2O, diethylether, and *n*-hexane several times and dried at 110°C for 14 h in vacuum.

3. Results and discussion

The reactions for the synthesis of L_1H_2, L_2H_2, and L_3H_2 are given in scheme 1. The ligands, L_1H_2, L_2H_2, and L_3H_2, were obtained from the reaction of

anti-phenylchloroglyoxime, *anti*-monochloroglyoxime, *anti*-dichloroglyoxime and 1-(2-aminoethyl)piperazine. Excess Et_3N (triethylamine) was used to neutralize the HCl liberated in the reaction. The analytical data of $[M(L_xH)_2]$ complexes indicate 1 : 2 metal to ligand stoichiometry. Additional analytical data are given tables 1–4.

The red colour of the Ni(II) complexes of L_1H_2, L_2H_2, and L_3H_2 indicates that the ligands are in the (*E*, *E*) form, [23, 24] (*anti*-form).

3.1. *NMR results*

The ^{1}H-NMR spectral results obtained for L_1H_2 and L_2H_2 with their Ni(II) complexes in DMSO or $CDCl_3$, together the assignments, are given in experimental section. In the ^{1}H-NMR spectrum of L_1H_2, there is deuterium exchangeable a broad signal at $\delta = 11.40$ ppm due to the $-$OH protons. In the ^{1}H-NMR spectrum of L_2H_2, two signals are observed for the protons since the $-$OH protons of the oxime groups are not equivalent [8, 25]. In L_2H_2, the chemical shifts of $-$OH protons are observed at about 10.52 and 10.14 ppm as singlets. In the ^{1}H-NMR spectrum of L_1H_2 and L_2H_2, the deuterium exchangeable proton of NH group appears as doublet at $\delta = 5.62$–5.80 ppm for L_1H_2 and as singlet $\delta = 5.54$ ppm, respectively. In the ^{1}H-NMR spectrum of $[Ni(L_1H)_2]$ and $[Ni(L_2H)_2]$, only slight differences between those of the ligands (L_1H_2 and L_2H_2) and their Ni(II) complexes were observed. While the chemical shifts of D_2O exchangeable NH protons were observed at $\delta = 5.76$ ppm for $[Ni(L_1H)_2]$ and $\delta = 5.31$ ppm for $[Ni(L_2H)_2]$, the intramolecular hydrogen bridging O–H · O protons have been shifted to a lower field at $\delta = 15.62$ ppm for $[Ni(L_1H)_2]$ and at $\delta = 14.42$ ppm for $[Ni(L_2H)_2]$, respectively as expected [4, 24].

In the ^{13}C-NMR spectrum of L_2H_2, the carbon resonances of oxime groups are observed at 139.0 (C_6), 153.7 (C_5) ppm. These non-equivalent carbon atoms, particularly, belong to hydroxyimino carbon atoms, also confirm the *anti* structure of L_2H_2 [26].

3.2. *IR results*

The characteristic infrared spectrum data are given table 2. The broad bands within the range 3110–3647 cm^{-1} for L_1H_2 and 3108–3605 cm^{-1} for L_2H_2 can be attributed to stretching vibrations of free υ(OH/NH) and intramolecular H-bonding. The observed negative shift of υ(C=N) stretching in the IR spectra of $M(L_xH)_2$ complexes (1615–1632 cm^{-1}) relative to free L_xH ligands (1633–1638 cm^{-1}) indicates the participation of the azomethine nitrogen atom of the ligands in coordination with the Ni(II), Co(II), and Cu(II) ions. The IR spectra of $M(L_xH)_2$ metal complexes were characterized by the appearance of very significant absorption band in the region 1730–1775 cm^{-1} due to υ(O–H · O) [27]. A sharp band observed between 964–990 cm^{-1} in ligands and metal complexes is assigned to the υ(N–O) vibration. The shifts of N–O absorbances to lower energy are consistent with the protonation occurring at the hydrogen-bridged oxime oxygen atoms, yielding a covalent O–H bond. The formation of OH bonds results in the removal of electron density from N–O bond and corresponding increase in the N–O bond lengths and decreased NO stretching vibrations [28]. The υ(O–H) stretching band observed at 3110–3647 cm^{-1} and 3108–3605 cm^{-1} in the IR spectrum of L_1H_2 and L_2H_2 together with the existence of

Table 1. The formula, formula weight, colours, melting points, molar conductivity yields, magnetic susceptibilities, and elemental analyses results of the compounds.

Compounds	F.W ($g\,mol^{-1}$)	Colour	M.p. (°C)	Λ_M ($\Omega^{-1}cm^2\,mol^{-1}$)	Yield (%)	μ_{eff} [B.M]	Elemental analyses % calculated (found) C	H	N
Ligand (L_1H_2) $C_{14}H_{21}N_5O_2$	291	Pale yellow	125	–	68	–	57.73 (56.18)	7.21 (7.62)	24.05 (23.54)
$Co(L_1H)_2 \cdot 2H_2O$ $C_{28}H_{44}N_{10}O_6Co$	675	Brown	293	3.8	65	3.89	49.77 (48.94)	6.52 (6.23)	20.74 (19.89)
$Cu(L_3H)_2$ $C_{28}H_{40}N_{10}O_4Cu$	644	Dark green	195	4.1	70	1.73	52.17 (51.65)	6.21 (5.76)	21.74 (22.07)
$Ni(L_3H)_2$ $C_{28}H_{40}N_{10}O_4Ni$	639	Green	252	4.6	74	Dia	52.58 (51.04)	6.23 (5.72)	21.90 (22.16)
Ligand ($L_2H)_2$ $C_8H_{17}N_5O_2$	219	Dirty white	123	–	80	–	43.83 (44.32)	7.76 (8.15)	31.96 (32.10)
$Co(L_2H)_2 \cdot 2H_2O$ $C_{16}H_{36}N_{10}O_6Co$	523	Brown	233	5.1	71	2.26	36.71 (36.64)	6.88 (6.43)	26.77 (26.38)
$Cu(L_2H)_2$ $C_{16}H_{32}N_{10}O_4Cu$	492	Green	140	5.8	65	1.82	39.02 (38.74)	6.50 (6.24)	28.45 (27.82)
$Ni(L_2H)_2$ $C_{16}H_{32}N_{10}O_4Ni$	487	Red	205	4.7	68	Dia	39.42 (39.26)	6.57 (6.32)	28.74 (28.36)
$Co(L_3H)_2 \cdot 2H_2O$ $C_{28}H_{62}N_{16}O_6Co$	777	Brown	>300	4.2	58	4.28	43.24 (42.93)	7.98 (7.60)	28.83 (28.56)
$Cu(L_3H)_2$ $C_{28}H_{58}N_{16}O_4Cu$	745	Green	180	4.6	63	1.84	45.10 (44.81)	7.79 (7.48)	30.06 (29.82)
$Ni(L_3H)_2 \cdot 2H_2O$ $C_{28}H_{58}N_{16}O_4Ni$	777	Red	>300	3.8	64	2.84	43.24 (43.08)	7.98 (7.61)	28.82 (28.07)

Table 2. Characteristic IR bands (cm^{-1}) of the ligands and complexes as KBr pellets.

Compounds	O–H/N–H	Aliph. C–H	O–H · O	N–O	C=N
Ligand, L_1H_2	3110–3647	2850–2956	–	988	1638
$Co(L_1H)_2 \cdot 2H_2O$	3137–3671	2835–2948	1769	968	1615
$Cu(L_1H)_2$	3096–3553	2858–2942	1757	964	1618
$Ni(L_1H)_2$	3125–3564	2811–293	1775	967	1615
Ligand, L_2H_2	3108–3605	2846–2954	–	990	1633
$Co(L_2H)_2 \cdot 2H_2O$	3125–3653	2865–2971	1730	970	1621
$Cu(L_2H)_2$	3078–3623	2847–2966	–	968	1632
$Ni(L_2H)_2$	3114–3629	2859–2936	1734	968	1630
$Co(L_3H)_2 \cdot 2H_2O$	3054–3653	2835–2964	–	982	1624
$Cu(L_3H)_2$	3048–3623	2847–2960	–	982	1618
$Ni(L_3H)_2$	3037–3647	2850–2925	–	997	1627

Table 3. Characteristic UV-Vis bands of the ligands and complexes.

Compounds	Solvents	Wavelength (λ_{max} (nm)) ($\log \varepsilon$, $M^{-1} cm^{-1}$)				
Ligand, L_1H_2	DMSO	228(5.56)	265(4.37)			
$Co(L_1H)_2 \cdot 2H_2O$	DMSO	215(4.18)	260(3.71)	510(2.15)	680*(1.78)	
$Cu(L_1H)_2$	DMSO	227(4.74)	265*(3.84)	527(2.42)	628(2.11)	
$Ni(L_1H)_2$	DMSO	217(3.89)	248(3.15)	470(2.85)	562(2.09)	
Ligand. L_2H_2	DMSO	210(5.44)	243(4.61)	275(3.75)		
$Co(L_2H)_2 \cdot 2H_2O$	DMSO	211(5.34)	237(4.21)	276(3.36)	310(3.04)	643(1.89)
$Cu(L_2H)_2$	DMSO	224(4.75)	240(4.13)	269(3.72)	638(2.03)	
$Ni(L_2H)_2$	DMSO	234(5.19)	273(4.42)	472(3.18)	558(2.14)	
$Co(L_3H)_2 \cdot 2H_2O$	DMSO	286(4.62)	346(3.21)	427(2.06)	638(1.84)	
$Cu(L_3H)_2$	DMSO	276(4.18)	350* (3.83)	372(3.26)	445(2.74)	641(2.03)
$Ni(L_3H)_2 \cdot 2H_2O$	DMSO	273(4.73)	361*(4.30)	419(3.30)	562(2.13)	

*Shoulder.

a H-bridge (O–H · O) at near 1730–1775 cm^{-1} and the shifting of υ(C=N) and υ(N–O) stretching in IR spectra of the $Ni(L_1H)_2$, $Ni(L_2H)_2$ and $Ni(L_1H)_2Cu(L_xH)_2$ complexes provide support for MN_4-type coordination in the complexes, whereas $Ni(L_3H)_2$ and $Co(L_xH)_2$ complexes provide support for $MN_4 \cdot 2H_2O$-type coordination in the complexes.

3.3. *UV-Vis results*

The characteristic UV-Vis spectrum data are given in table 3. The UV-Vis spectra of the ligands (L_1H_2 and L_2H_2) in DMSO showed two absorption bands between 228–265 nm for L_1H_2, three absorption bands between 210–275 nm for L_2H_2, respectively. The UV-Vis spectra of the Cu(II), Ni(II), and Co(II) complexes in DMSO showed absorption bands between 210–680 nm. Each complex shows several absorption bands in the UV-Vis region. The absorptions in the ultraviolet region are assignable to transitions involving ligands orbitals [29]. The absorption bands below 276 nm are practically identical and can be attributed to $\pi \rightarrow \pi^*$ transitions in the benzene ring and azomethine (–C=N) groups. The absorption bands observed within the range of 310–372 nm is most probably due to the transition of $n \rightarrow \pi^*$ of imine group

Table 4. Voltametric data for the complexes in DMSO–TBAP.

Complexes	M^{2+}/M^{3+} $E_{1/2}$[a] (V)	ΔE_p[b] (V)	I_{pa}/I_{pc}[c]	M^{2+}/M^{+} $E_{1/2}$[a] (V)	ΔE_p[b](V)	I_{pa}/I_{pc}[c]	L/L^{-} $E_{1/2}$[a] (V)	ΔE_p[b] (V)	I_{pa}/I_{pc}[c]	L/L^{+} $E_{1/2}$[a] (V)	ΔE_p[b] (V)	I_{pa}/I_{pc}[c]
$[Ni(L_1H)_2]$				−0.683	0.080	0.23	−1.19	0.060	0.38	0.560		
$[Ni(L_2H)_2]$	0.185						−1.15			0.699	0.200	0.40
$[Co(L_1H)_2]$	0.325	0.150	0.93	−0.383	0.160	0.12	−1.03			1.23		
$[Co(L_2H)_2]$	0.305	0.090	0.93	−0.785	0.350	1.07						
$[Cu(L_1H)_2]$	0.055			−0.470	0.290		−0.89			0.405	0.28	1.60
$[Cu(L_2H)_2]$	0.268	0.410	0.42	−0.685	0.410	0.53	−1.25			0.621	0.480	0.72

[a]Cathodic peak potential for reduction, anodic peak potential for oxidation for irreversible processes.
[b]$\Delta E_p = E_{pc} - E_{pa}$ at 0.100 V s^{-1} scan rate.
[c]i_{pa}/I_{pc} for reduction, I_{pc}/I_{pa} for oxidation at 0.100 V s^{-1} scan rate.

corresponding to the ligands or complexes [30]. The absorption bands at 419 and 527 nm are assigned to metal-to-ligand charge transfer (MLCT) and $^1A_{1g} \rightarrow {}^1B_{1g}$ transitions [31], respectively. The electronic spectra of Cu(II) complexes in DMSO show a broad band at 628 nm for $Cu(L_1H)_2$, 638 nm for $Cu(L_2H)_2$, and 641 nm for $Cu(L_3H)_2$, which assign to $^2E_g \rightarrow {}^2T_{2g}$ transitions, characteristic for square planar geometry [32]. The weak d–d transitions of square planar Ni(II) complexes were observed in the between 419–568 nm [33]. The weak d-d metal absorption bands were observed in DMSO at 680 nm for $Co(L_1H)_2$, 643 nm for $Co(L_2H)_2$, and 638 nm for $Co(L_3H)_2$, respectively (table 3).

3.4. *Magnetic moments*

Magnetic moments measurements of compounds carried out at 25°C show that $[Ni(L_1H)_2]$ and $[Ni(L_2H)_2]$ complexes are diamagnetic, indicating the low-spin ($S = 0$) square planar d^8-systems, whereas $[Ni(L_3H)_2 \cdot 2H_2O]$ complex is paramagnetic ($\mu_{eff} = 2.84$ BM), indicating the the high-spin ($S = 1$) octahedral d^8-systems, as expected. The absorption bands observed for the electronic spectra of Ni(II) complexes also support the square planar or octahedral geometry for Ni(II) complexes [34] (table 3). The cobalt(II) and copper(II) complexes are paramagnetic. Their magnetic susceptibilities are 3.89 BM (high-spin) for $Co(L_1H)_2$, 2.26 BM (low-spin) for $Co(L_2H)_2$, and 4.28 (high-spin) BM for $Co(L_3H)_2$ with 1.73 BM for $Cu(L_1H)_2$, 1.82 BM for $Cu(L_2H)_2$, and 1.84 BM for $Cu(L_2H)_2$, respectively. According to these results, a square-planar geometry for the copper(II) complexes, and an octahedral geometry for the cobalt(II) complex are proposed [34b, 35]. The cobalt(II) complexes axially coordinated two water molecules were also characterized by the IR spectrum and elemental analysis. The observation of the $(O-H \cdot O)$ bond leads us to consider the geometry of complexes to be octahedral [35]. The UV-Vis spectra of the Co(II) and Cu(II) complexes supported these structures due to the observation of $\pi \rightarrow \pi^*$ and d–d transitions (table 3). The structures of the metal complexes proposed are shown in figure 1.

3.5. *Electrochemical results*

The electrochemical behaviour of the new dioxime complexes, $[M(L_1H)_2]$ and $[M(L_2H)_2]$, where M = Ni(II), Co(II), and Cu(II) ions, were investigated using cyclic voltammetric (CV) technique in DMSO solution containing 0.1 M TBAP. The data collected in this work are summarized in table 4. As seen from figure 2(a), the $[Ni(L_1H)_2]$ complex displayed two reduction peaks at −0.683 and −1.19 V *versus* Ag/AgCl with the corresponding anodic waves on the reverse scan (table 4). The peak separations of the first and second reduction processes are 0.080 and 0.060 V at 0.100 V s^{-1} scan rate, which assign to reversible wave for the electron transfer reactions. The low values of the anodic-to-cathodic peak current for each steps should be considered as a chemical reaction during electron transfer on the electrode surface. This complex also exhibited irreversible ligand-based oxidation process without corresponding cathodic peak. Figure 2(b) shows the CV of the $[Ni(L_2H)_2]$ complex, where it displayed two irreversible reduction and two irreversible oxidation processes. As could be seen from figure 2(b), the first reduction wave based on the metal ion coincides with the second reduction wave based on the oxime moity, resulting a broad peak (Ic, IIc) in

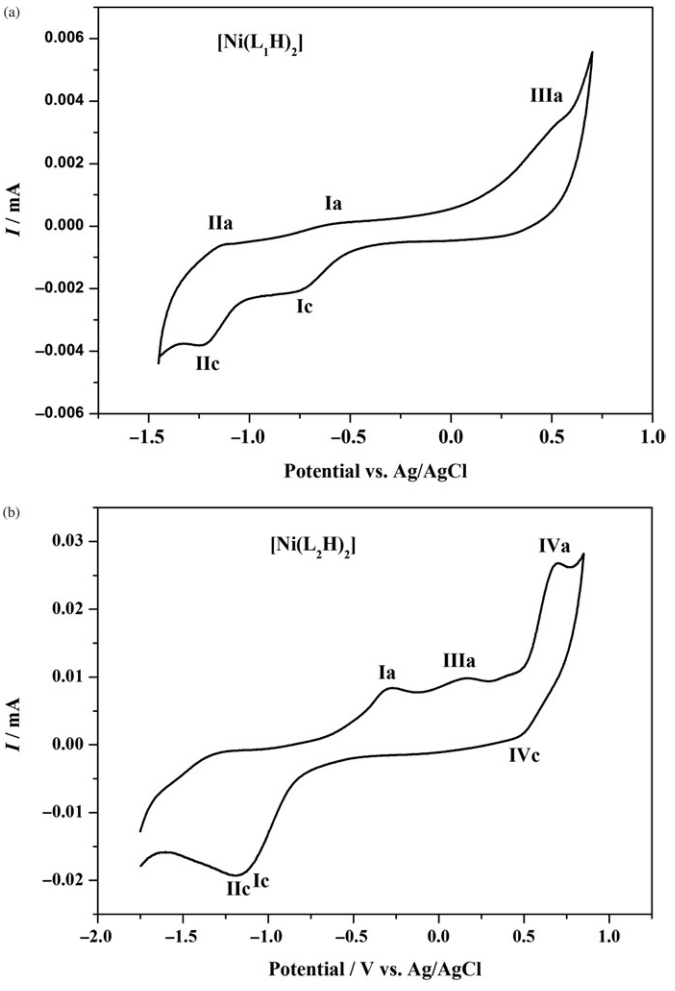

Figure 2. Cyclic voltammograms of (a) $[Ni(L_1H)_2]$, and (b) $[Ni(L_2H)_2]$, complexes in DMSO/0.1 M TBAP at 0.100 V s^{-1} scan rate.

the cathodic side. Re-oxidation peak (Ia) corresponding to the first reduction peak was observed at −0.304 V. The cathodic and anodic peak potentials for the reduction and the oxidation processes are located at −1.15, 0.185, and 0.699 V, respectively. It is concluded from these results that the electrochemical behaviour of the $[Ni(L_2H)_2]$ complex is not similar to that of the $[Ni(L_1H)_2]$ complex. The oxidation step with the metal-based character which was observed for the $[Ni(L_2H)_2]$ complex could not be detected for the $[Ni(L_2H)_2]$ complex. Also, the reversible reduction waves observed for the $[Ni(L_1H)_2]$ complex was observed as irreversible in the case of the $[Ni(L_2H)_2]$ complex. This behaviour could be attributed to the instability of reduced species in the case of the $[Ni(L_2H)_2]$ complex having a different environment with respect to the $[Ni(L_1H)_2]$ complex. Figure 3(a) shows the CV of the $[Co(L_1H)_2]$ complex which displayed two reduction and two oxidation peaks located at −0.383, −1.03, 0.325, and 1.23 V, respectively. The first peaks observed in the cathodic and anodic sides assign to metal-based processes with the formation of Co(II)/Co(I) mono-anionic and

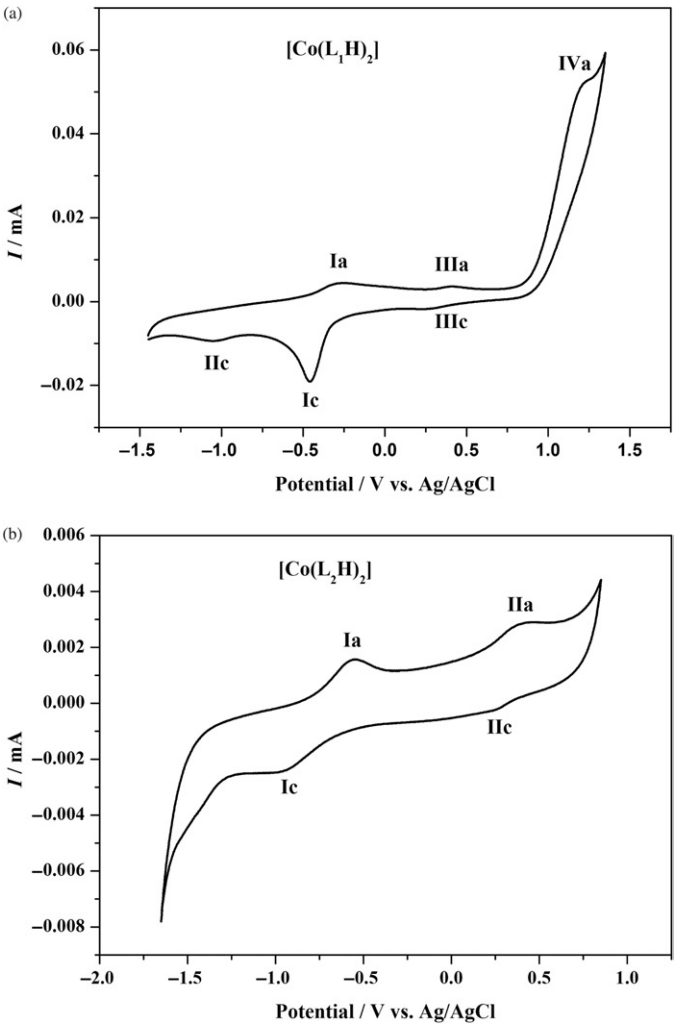

Figure 3. Cyclic voltammograms of (a) $[Co(L_1H)_2]$, and (b) $[Co(L_2H)_2]$, complexes in DMSO/0.1 M TBAP at 0.100 V s^{-1} scan rate.

Co(III)/Co(II) mono-cationic species as previously observed for the cobalt dioxime complexes [36–39]. Electron transfer reaction of the first reduction process proceeds with the adsorption mechanism due to the existence of high peak current (Ic) with respect to the other peak current (IIc and IIIc). The proportional increasing of the peak current corresponding to the (Ic) with the increasing scanning rate indicates adsorption character of the wave for the first reduction process [40, 41]. The second reduction and oxidation steps exhibit irreversible wave due to lack of corresponding anodic waves, which are based on the oxime moieties, as expected. It can be seen from figure 3(a) that the high anodic peak current (IVa) observed for the $[Co(L_1H)_2]$ complex is caused by the background current originated from the solvent. Figure 3(b) shows the CV of the $[Co(L_2H)_2]$ complex which displayed one quasi-reversible reduction and one quasi-reversible oxidation waves. The reduction and oxidation processes assign to

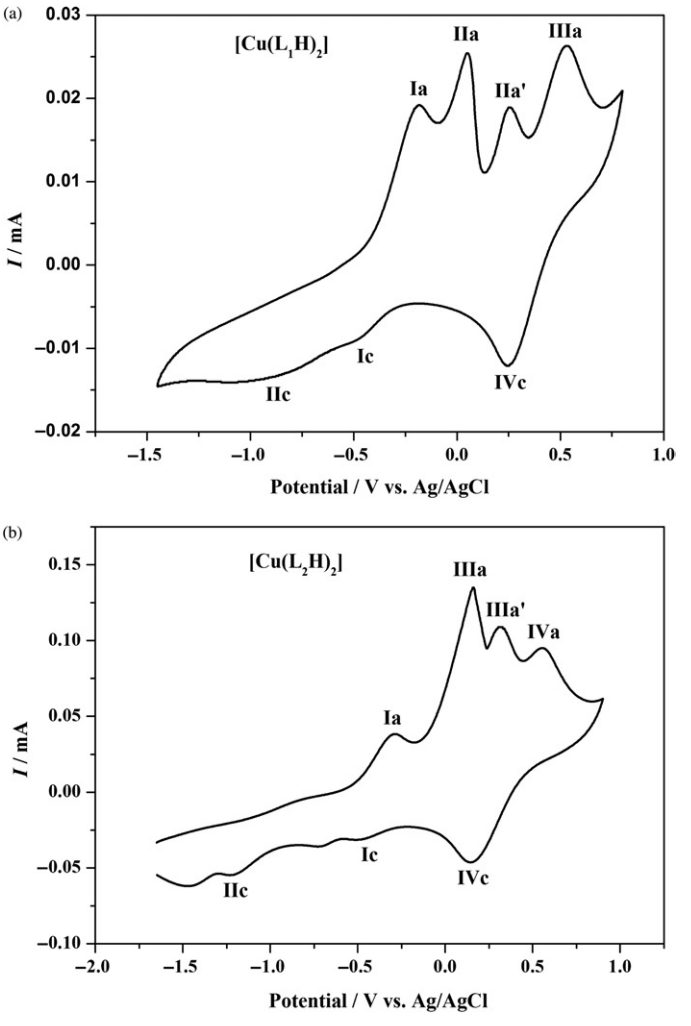

Figure 4. Cyclic voltammograms of (a) $[Cu(L_1H)_2]$, and (b) $[Cu(L_2H)_2]$, complexes in DMSO/0.1 M TBAP at 0.100 V s^{-1} scan rate.

metal-based Co(II)/Co(I) and Co(III)/Co(II) species, half-wave potentials of which are located at −0.785 and 0.305 V, respectively. It is concluded from the result that the electrode potentials of the reduction species for the $[Co(L_1H)_2]$ anodically shift compared to that of the $[Co(L_1H)_2]$ complex in the same experimental condition. It could be attributed to the electron-donating effect of the phenyl groups substituted on the oxime moity of the $[Co(L_1H)_2]$ complex. The same effect is probably responsible for the cathodic shift of the oxidation potentials of the $[Co(L_1H)_2]$ complex and the absence of ligand-based oxidation or reduction reactions of the $[Co(L_2H)_2]$ within the available solvent potential window as previously observed for some phthalocyanines [42–46]. $[Cu(L_1H)_2]$ and $[Cu(L_2H)_2]$ complexes showed interesting electrochemical behaviour on the electrode surface (figure 4). The CV of the $[Cu(L_1H)_2]$ complex exhibited irreversible two reduction waves having metal-based with Cu(II)/Cu(I) mono-anionic and ligand-based di-anionic species, respectively. The adsorption waves

corresponding to the first oxidation based on the formation of Cu(II)/Cu(III) species was observed on the electrode surface, to which the proportional increasing of anodic peak currents (IIa and IIIa) with increasing scan rates provides satisfactory evidence for the adsorption character of wave for the electron transfer mechanism. As seen from figure 4(a), the anodic peak corresponding to the Cu(II)/Cu(III) species is split into two different cathodic waves (IIa, IIa'), one of which (IIa) corresponds to adsorption character and the other one (IIa') is responsible for the diffusion-controlled transfer mechanism in the solution. The best evidence for this behaviour was provided with the peak current ratio of each anodic waves (IIa and IIa'). As could be expected, the peak current formed in the courses of oxidation in the solution is lower than that observed on the electrode surface with the adsorbed mechanism. The first oxidation process displayed irreversible character due to lack of corresponding the cathodic peak. The similar electrochemical behaviour of second oxidation wave at 0.405 V was observed for the copper complex. This wave is based on the ligand character and irreversible with the high peak separation and high peak current ratio. Figure 4(b) gives the CV of the $[Cu(L_2H)_2]$ complexes, which displayed two irreversible reduction and two irreversible oxidation processes. Their cathodic and anodic peak potentials are listed in table 4. As expected, this complex exhibited similar electrochemical behaviour with what was observed for the $[Cu(L_1H)_2]$ complex. The shifts observed in the electrode potentials probably come from different environment of the $[Cu(L_2H)_2]$ complex as observed in the cases of the nickel and cobalt complexes studied in this work.

Acknowledgements

This work have been supported, in part, by the Turkish Academy of Sciences in the framework of the Young Scientist Award Program (EA-TÜBA-GEBİP/2001-1-1), and The Research Fund of Harran University (Sanliurfa, Turkey).

References

[1] U.S. Vural, H.C. Sevindir. *Macromol. Rep*., **A31**(Suppl. 5), 673 (1994).
[2] R.C. Mehrotra. In *Comprehensive Coordination Chemistry*, G. Wilkinson, R.D. Gillard, J.A. McCleverty (Eds), p. 269, Pergamon Press, New York (1988).
[3] A. Chakravorty. *Coord. Chem. Rev*., **13**, 1 (1974).
[4] A. Gül, Ö. Bekaroğlu. *J. Chem. Soc. Dalton Trans*., 2537 (1983).
[5] Y. Gök, Ö. Bekaroğlu. *Synth. React. Inorg. Met.-Org. Chem*., **11**, 621 (1981).
[6] V. Ahsen, F. Gokceli, O. Bekaroğlu. *J. Chem. Soc. Dalton Trans*., 1827 (1987).
[7] E. Özcan, R. Mirzaoğlu. *Synth. React. Inorg. Met.-Org. Chem*., **18**, 559 (1988).
[8] E. Tas, M. Ulusoy, M. Guler. *Synth. React. Inorg. Met.-Org. Chem*., **37**(7), 1221 (2004).
[9] V.I. Ovcharenko, S.V. Fokin, V.A. Reznikov, V.V. Ikorskii, G.V. Romanenko, R.Z. Sagdeev. *Inorg. Chem*., **37**, 2104 (1998).
[10] D. Xu, J. Gu, L. Xu, K. Liang, Y. Xu. *Polyhedron*, **17**, 231 (1998).
[11] F. Birkelbach, T. Weyhermuller, M. Lengen, M. Gerdan, A.X. Trautwein, K. Wieghardt, P. Chaudhuri. *J. Chem. Soc. Dalton Trans*., 4529 (1997).
[12] V.E. Zavodnik, V.K. Belsky, Y.Z. Voloshin, O.A. Varzatsky. *J. Coord. Chem*., **23**, 97 (1993).
[13] J.H. Pratt. *Inorganic Chemistry of Vitamin B-12*, Academic Press, New York (1972).

[14] (a) G.N. Schrauzer. *Accs. Chem. Res.*, **1**, 97 (1968); (b) G.N. Schrauzer. *Angew. Chem. Int. Ed. Eng.*, **15**, 417 (1976).
[15] L.A. Tschugaev. *Z. Anorg. Chem.*, **46**, 144 (1905).
[16] M.J. Prushan, A.W. Addison, R.J. Butcher. *Inorg. Chem. Acta*, **300**, 992 (2000).
[17] (a) F.L. Loret, R. Ruiz, B. Cervera, I. Castro, M. Julve, J. Faust, J.A. Real, F. Sapina, Y. Journaux, J.C. Colin, M. Vandager. *J. Chem. Soc., Chem. Commun.*, **22**, 2615 (1994); (b) D. Luneau, H. Oshio, H. Okawa, S Kida, *J. Chem. Soc. Dalton Trans.*, 2283 (1990).
[18] H. Britzingen, R. Titzmann. *Ber. Dtsch. Chem. Ges.*, **85**, 345 (1952).
[19] G. Panzio, F. Baldracco. *Gazz. Chim. Ital.*, **60**, 415 (1930).
[20] A. Earnshaw. *Introduction to Magnetochemistry*, p. 4, Acedemic Press, London (1968).
[21] U. Brand, H. Vahrenkamp. *Chem. Ber.*, **129**, 435 (1996).
[22] Z. Zhang, A.E. Martell, R.T. Motekaitis, L. Fu. *Tetrahed. Lett.*, **40**, 4615 (1999).
[23] M. Kurtoglu, S. Serin. *Synth. React. Inorg. Met.-Org. Chem.*, **31**(7), 1129 (2001).
[24] S.B. Pedersen, E. Larsen. *Acta Chem. Scand.*, **27**, 3291 (1973).
[25] H.I. Ucan, R. Mirzaoglu. *Synth. React. Inorg. Met.-Org. Chem.*, **20**, 437 (1990).
[26] Y. Gök, H. Kantekin, H. Alp, M. Özdemir. *Z. Anorg. Allg. Chem.*, **621**, 1237 (1995).
[27] (a) Y. Gök, S. Karaböcek, N. Karaböcek, Y. Atalay. *New J. Chem.*, **19**, 1275 (1995) (b) M.S. Hussain, H.M. Al-Mohdhar, A.R. Al-Arfaj. *J. Coord. Chem.*, **18**, 339 (1988) (c) E. Tas, M. Aslanoglu, A. Kilic, Z. Kara. *Trans. Met. Chem.*, **30**, 758 (2005).
[28] Y. Gök, A. Bilgin, H. Ertepinar, E. Nisanoglu. *Indian J. Chem.*, **39A**, 1280 (2000).
[29] A.K. Das, S.M. Perg, S. Bhattacharya. *Polyhedron*, **20**, 327 (2001).
[30] C. Fraser, B. Bosnich. *Inorg. Chem.*, **33**, 338 (1994).
[31] A.B.P. Lever. *Inorganic Electronic Spectroscopy*, Elsevier, Amsterdam (1984).
[32] R.L. Carlin. *Transition Metal Chemistry*, Marcel Dekker, New York (1965).
[33] (a) G. Maki. *J. Phys. Chem.*, **28**, 651 (1958); (b) H. Gary, C.J. Ballhausen. *J. Am. Chem. Soc.*, **85**, 260 (1963).
[34] (a) V. Ahsen, A. Kürek, A. Gül, M. Ö. Bekaroğlu. *J. Chem. Soc. Dalton Trans.*, 5 (1990); (b) V. Ahsen, Ö. Bekaroğlu. *Synth. React. Inorg. Met.-Org. Chem.*, **15**, 61 (1985); (c) A.N. Sing, A. Chakravorty. *Inorg. Chem.*, **19**, 969 (1980).
[35] F.A. Cotton, G. Wilkinson. *Advanced Inorganic Chemistry, The Elements of the First Transition Series*, A. Wiley-Interscience Publication, John Wiley and Sons, New York (1988).
[36] M. Kandaz, I. Yilmaz, S. Keskin, A. Koca. *Polyhedron*, **21**, 825 (2002).
[37] M. Kandaz, S.Z. Coruhlu, I. Yilmaz, A.R. Ozkaya. *Transit. Metal. Chem.*, **27**, 877 (2002).
[38] I. Yilmaz, M. Kandaz, A.R. Özkaya, A. Koca. *Monatsh. Chem.*, **133**, 609 (2002).
[39] E. Tas, M. Ulusoy, M. Guler. *Transit. Metal. Chem.*, **29**, 180 (2004).
[40] A.J. Bard, L.R. Faulkner (Eds). *Electrochemical Methods: Fundamentals and Applications*, 2nd Edn, p. 228, John Wiley & Sons, New York (2001).
[41] A.R. Özkaya, I. Yilmaz, O. Bekaroğlu. *J. Porhyr. Phthalocya.*, **2**, 483 (1998).
[42] K.M. Kadish, T. Nakanishi, A.G. Gürek, V. Ahsen, I. Yilmaz. *J. Phys. Chem. B*, **105**, 9817 (2001).
[43] I. Yilmaz, T. Nakanishi, A. Gürek, K.M. Kadish. *J. Porhyr. Phthalocya.*, **7**, 227 (2003).
[44] T. Nakanishi, I. Yilmaz, N. Nakashima, K.M. Kadish. *J. Phys. Chem. B*, **107**, 12789 (2003).
[45] I. Yilmaz, M. Kocak. *Polyhedron*, **23**, 1279 (2004).
[46] I. Yilmaz, A.G. Gurek, V. Ahsen. *Polyhedron*, **24**, 791 (2005).